JCTC Journal of Chemical Theory and Computation

pubs.acs.org/JCTC Article

# Global Hybrid Multiconfiguration Pair-Density Functional Theory

Mohammad Mostafanejad, Marcus Dante Liebenthal, and A. Eugene DePrince III*

**Cite This:** *J. Chem. Theory Comput.* 2020, 16, 2274−2283 Read Online

ACCESS | Metrics & More | Article Recommendations | Supporting Information

**ABSTRACT:** A global hybrid extension of multiconfiguration pair-density functional theory (MC-PDFT) is developed. Using a linear decomposition of the electron−electron repulsion term, a fraction $\lambda$ of the nonlocal exchange interaction, obtained from variational two-electron reduced-density matrix (v2RDM)-driven complete active-space self-consistent field (CASSCF) theory, is combined with its local counterpart, obtained from an on-top pair-density functional. The resulting scheme (called $\lambda$-MC-PDFT) inherits the benefits of MC-PDFT (e.g., its simplicity and the resolution of the symmetry dilemma) and, when combined with the v2RDM approach to CASSCF, requires only polynomially scaling computational effort. As a result, $\lambda$-MC-PDFT can efficiently describe static and dynamical correlation effects in strongly correlated systems. The efficacy of the approach is assessed for several challenging multiconfigurational problems, including the dissociation of molecular nitrogen, the double dissociation of a water molecule, and the 1,3-dipolar cycloadditions of ozone to ethylene and ozone to acetylene in the O3ADD6 benchmark set.

## 1. INTRODUCTION

The search for a universally accurate and efficient delineation of electron correlation effects is an active area of research in modern electronic structure theory.[1,2] For strongly correlated systems, in particular, where the multiconfigurational character of the wave function cannot be ignored, the single-determinant form of Kohn−Sham density functional theory (DFT)[3,4] will fail, often dramatically so. In such cases, a possible remedy is to combine multireference and DFT methods (MR+DFT) to separately model strong and weak correlation effects, respectively.[5−34] The development of multiconfiguration pair-density functional theory (MC-PDFT)[27] represents an important step in this direction, as this approach effectively capitalizes on the complementary strengths of complete active-space self-consistent field (CASSCF) theory[35−38] and DFT to offer a robust description of nondynamic correlation effects and an economical representation of dynamical correlation. Moreover, MC-PDFT resolves Kohn−Sham DFT's symmetry dilemma by relying on functionals of the total density and the on-top pair-density (OTPD)[26,27,39] (as opposed to functionals of the spin-density). The approach also avoids double counting the electron correlation by retaining only the classical Coulomb electron−electron repulsion energy from CASSCF and relying on OTPD functionals for the nonclassical contributions. Recently, we presented[40] a reduced-density matrix (RDM)-based formulation of MC-PDFT that retains these nice properties while significantly reducing the computational cost of the underlying CASSCF calculations through the direct variational optimization[41] of the active-space two-electron RDM (2-RDM).[42,43] As such, variational 2-RDM (v2RDM)-driven MC-PDFT can be applied to challenging multireference problems that require the consideration of large active spaces.

Because commonly used[26,27] OTPD functionals and their conventional Kohn−Sham DFT counterparts differ only in the input densities (as opposed to their actual functional forms), MC-PDFT includes some of the same functional error that is responsible for the delocalization error[44] that plagues familiar local spin density approximation and generalized gradient approximation exchange-correlation (XC) functionals in Kohn−Sham DFT.[45−49] This delocalization error arises because the electron-gas model[50] leads to an incorrect picture of the noninteracting limit, in which the Coulomb repulsion coupling strength is zero. The global hybrid scheme offers the simplest remedy for delocalization error by replacing a fraction of the electron-gas exchange with its exact (Hartree−Fock) counterpart, which then leads to the correct noninteracting limit.[45−49] Unlike Kohn−Sham DFT, MC-PDFT is not a self-consistent theory, which means that MC-PDFT will be free from delocalization error,[51] provided that the total density and OTPD that enter the OTPD functionals have the correct physical behavior. Nonetheless, the OTPD functionals commonly used within MC-PDFT still contain the same

**Received:** November 25, 2019
**Published:** February 26, 2020

https://dx.doi.org/10.1021/acs.jctc.9b01178

functional error that leads to delocalization error in Kohn−Sham DFT.

In light of the great success of the global hybrid scheme in standard Kohn−Sham DFT, several proposals have been offered that extend this approach to the multiconfiguration regime;[29−34] for a survey of these techniques, the reader is referred to ref 28. The present study is inspired by the multiconfiguration one-parameter hybrid density functional theory (MC1H) method of Sharkas et al.,[30] which is similar to MC-PDFT in that it captures nondynamical correlation with multiconfiguration self-consistent field (MCSCF) theory and the remaining dynamical correlation effects via DFT. The MC1H method has motivated the development of other MR+DFT techniques, such as pair coupled-cluster doubles $\lambda$DFT (pCCD-$\lambda$DFT)[31,32] and $\lambda$-density functional valence bond ($\lambda$-DFVB),[33] where $\lambda$ refers to the hybrid parameter that controls the admixture of nonlocal exchange effects. Through this parameter, both pCCD-$\lambda$DFT and $\lambda$-DFVB can interpolate between DFT and a MR scheme (i.e., pCCD or VB).[29,34] In this work, we follow the general strategy proposed in refs 30 and 52 to realize a global hybrid MC-PDFT formalism that reduces OTPD functional error through the admixture of nonlocal exchange; we term this approach $\lambda$-MC-PDFT. $\lambda$-MC-PDFT differs from the MC1H approach that inspired it in two respects. First, $\lambda$-MC-PDFT is not a self-consistent theory, whereas MC1H is. Second, like pCCD-$\lambda$DFT (and unlike MC1H), $\lambda$-MC-PDFT relies on XC functionals of the total and on-top pair densities, rather than functionals of the total and spin densities.

The manuscript is organized as follows. Section 2 provides the theoretical details of $\lambda$-MC-PDFT. In section 3, we discuss the application of $\lambda$-MC-PDFT to the dissociation of molecular nitrogen and the symmetric double dissociation of a water molecule, as well as to the standard O3ADD6 benchmark set. Because we employ a v2RDM-driven formulation of $\lambda$-MC-PDFT, we explore the influence that the quality (i.e., the N-representability[53]) of the input RDMs has on the $\lambda$-MC-PDFT energy. Previous work[40] suggested that the results obtained from v2RDM-driven MC-PDFT were somewhat insensitive to the N-representability of the underlying RDMs, but we demonstrate in section 3 that the global hybrid scheme cleans up enough of the OTPD functional error that one can sometimes discern errors associated with approximately N-representable RDMs. Concluding remarks and potential future directions are then provided in section 4.

## 2. THEORY

Throughout this work, we use the conventional notation of MR methods when labeling the orbitals: the indices *i*, *j*, *k*, and *l* denote inactive (doubly occupied) orbitals; *t*, *u*, *v*, and *w* represent active orbitals; and *p*, *q*, *r*, and *s* indicate general orbitals. A summation over repeated indices is implied in all expressions.

We begin by defining the nonrelativistic Born−Oppenheimer electronic Hamiltonian

$$\hat{H} = h_q^p \hat{a}_{p_\sigma}^\dagger \hat{a}_{q_\sigma} + \frac{1}{2}\nu_{rs}^{pq} \hat{a}_{p_\sigma}^\dagger \hat{a}_{q_\tau}^\dagger \hat{a}_{s_\tau} \hat{a}_{r_\sigma} \tag{1}$$

where $\hat{a}^\dagger$ and $\hat{a}$ represent second-quantized creation and annihilation operators, respectively, and the Greek labels run over $\alpha$ and $\beta$ spins (the sum over which is implied). The symbol $h_q^p = \langle \psi_p | \hat{h} | \psi_q \rangle$ represents the sum of the electron kinetic energy and electron−nucleus potential energy integrals, and $\nu_{rs}^{pq} = \langle \psi_p \psi_q | \psi_r \psi_s \rangle$ is an element of the electron repulsion integral (ERI) tensor. Because the electronic Hamiltonian includes up to only pairwise interactions, the ground-state energy of a many-electron system can be expressed as an exact linear functional of the one-electron RDM (1-RDM) and the 2-RDM[54−56]

$$E = {}^1D_q^p h_q^p + \frac{1}{2} {}^2D_{rs}^{pq} \nu_{rs}^{pq} \tag{2}$$

Here, the 1-RDM and the 2-RDM are represented in their spin-free forms, with elements defined as

$${}^1D_q^p = {}^1D_{q_\sigma}^{p_\sigma} = \langle \Psi | \hat{a}_{p_\sigma}^\dagger \hat{a}_{q_\sigma} | \Psi \rangle \tag{3}$$

and

$${}^2D_{rs}^{pq} = {}^2D_{r_\sigma s_\tau}^{p_\sigma q_\tau} = \langle \Psi | \hat{a}_{p_\sigma}^\dagger \hat{a}_{q_\tau}^\dagger \hat{a}_{s_\tau} \hat{a}_{r_\sigma} | \Psi \rangle \tag{4}$$

respectively. Again, the summation over the spin labels in eqs 3 and 4 is implied.

The MC-PDFT expression for the electronic energy is

$$E_{\text{MC-PDFT}} = 2h_i^i + h_u^{t1} D_u^t + E_{\text{H}} + E_{\text{xc}}[\rho, \Pi, |\nabla\rho|, |\nabla\Pi|] \tag{5}$$

where $\rho(\mathbf{r})$ and $\Pi(\mathbf{r})$ are the total density and on-top pair density, respectively, and the Hartree energy, $E_{\text{H}}$, is defined as

$$E_{\text{H}} = 2\nu_{ij}^{ij} + 2\nu_{ui}^{ti1} D_u^t + \frac{1}{2}\nu_{uw}^{tv1} D_u^{t1} D_w^v \tag{6}$$

$E_{\text{xc}}$ represents either a translated (t)[27] or fully translated (ft)[57] OTPD XC functional. Given a total density and a spin density, $m(\mathbf{r})$, derived from a single Slater determinant, the spin polarization factor, $\zeta(\mathbf{r}) = m(\mathbf{r})/\rho(\mathbf{r})$, can be expressed as[39]

$$\zeta(\mathbf{r}) = \sqrt{1 - R(\mathbf{r})} \tag{7}$$

where

$$R(\mathbf{r}) = \frac{4\Pi(\mathbf{r})}{\rho^2(\mathbf{r})} \tag{8}$$

The basic assumption of translated OTPD functionals is that a similar relationship holds for arbitrary (i.e., correlated) densities, and thus the translated spin polarization factor can be defined as

$$\zeta_t(\mathbf{r}) = \begin{cases} \sqrt{1 - R(\mathbf{r})} & R(\mathbf{r}) \le 1 \\ 0 & R(\mathbf{r}) > 1 \end{cases} \tag{9}$$

In this way, $\zeta_t(\mathbf{r})$ can be used to construct an approximate spin density that enters a standard XC functional. Fully translated functionals are similarly defined with the distinction that they also depend upon the gradient of the OTPD. The interested reader is referred to ref 40 for additional details.

The total electronic density and its gradient that enter $E_{\text{xc}}$ are defined as

$$\rho(\mathbf{r}) = {}^1D_q^p \psi_p^*(\mathbf{r}) \psi_q(\mathbf{r}) \tag{10}$$

and

$$\nabla\rho(\mathbf{r}) = {}^1D_q^p [\nabla\psi_p^*(\mathbf{r}) \psi_q(\mathbf{r}) + \psi_p^*(\mathbf{r}) \nabla\psi_q(\mathbf{r})] \tag{11}$$

respectively. The OTPD and its gradient can similarly be expressed in terms of the 2-RDM as

$$\Pi(\mathbf{r}) = {}^2D^{pq}_{rs}\psi_p^*(\mathbf{r})\psi_q^*(\mathbf{r})\psi_r(\mathbf{r})\psi_s(\mathbf{r}) \tag{12}$$

and

$$\begin{aligned}\nabla\Pi(\mathbf{r}) = {}^2D^{pq}_{rs}[&\nabla\psi_p^*(\mathbf{r})\psi_q^*(\mathbf{r})\psi_r(\mathbf{r})\psi_s(\mathbf{r}) \\ &+ \psi_p^*(\mathbf{r})\nabla\psi_q^*(\mathbf{r})\psi_r(\mathbf{r})\psi_s(\mathbf{r}) \\ &+ \psi_p^*(\mathbf{r})\psi_q^*(\mathbf{r})\nabla\psi_r(\mathbf{r})\psi_s(\mathbf{r}) \\ &+ \psi_p^*(\mathbf{r})\psi_q^*(\mathbf{r})\psi_r(\mathbf{r})\nabla\psi_s(\mathbf{r})]\end{aligned} \tag{13}$$

respectively. In the MC-PDFT formalism, the 1-RDM and 2-RDM can be taken from any reference calculation capable of generating "good" RDMs that include nondynamical correlation effects. In this work, the 1-RDM and 2-RDM are taken from v2RDM-driven CASSCF calculations, and they satisfy either two-particle (PQG)[58] or PQG plus partial three-particle (T2)[59,60] N-representability conditions.

To reduce the functional error in the MC-PDFT formalism, we define the $\lambda$-MC-PDFT energy expression in which a fraction $\lambda \in (0, 1)$ of the OTPD exchange is replaced with contributions from the reference 1-RDM and 2-RDM

$$\begin{aligned}E_{\lambda\text{-MC-PDFT}} = {}& 2h^i_i + h^t_u\,{}^1D^t_u + E_\mathrm{H} \\ &+ \lambda\left(\frac{1}{2}\nu^{tv}_{uw}[{}^2\Delta^{tv}_{uw} - {}^1D^t_w\,{}^1D^v_u] - \nu^{tu}_{ii}\,{}^1D^t_u - \nu^{ii}_{jj}\right) \\ &+ \bar{E}^\lambda_\mathrm{xc}[\rho, \Pi, |\nabla\rho|, |\nabla\Pi|]\end{aligned} \tag{14}$$

Here, the two-cumulant, ${}^2\Delta$, is the part of the 2-RDM that cannot be represented in terms of the 1-RDM and is defined according to[61,62]

$${}^2D^{tv}_{uw} = {}^2\Delta^{tv}_{uw} + {}^1D^t_u\,{}^1D^v_w - {}^1D^t_w\,{}^1D^v_u \tag{15}$$

The complement OTPD functional, $\bar{E}^\lambda_\mathrm{xc}[\cdot]$, is given by

$$\begin{aligned}&\bar{E}^\lambda_\mathrm{xc}[\rho, \Pi, |\nabla\rho|, |\nabla\Pi|] \\ &\quad= E_\mathrm{xc}[\rho, \Pi, |\nabla\rho|, |\nabla\Pi|] - E^\lambda_\mathrm{xc}[\rho, \Pi, |\nabla\rho|, |\nabla\Pi|]\end{aligned} \tag{16}$$

which is the difference between the conventional exchange-correlation OTPD functional ($E_\mathrm{xc}[\cdot]$) and its $\lambda$-dependent hybrid version ($E^\lambda_\mathrm{xc}[\cdot]$).[30]

The exchange part of the complement functional is easily defined, as it simply scales linearly with the mixing parameter $\lambda$[29,30,52]

$$\bar{E}^\lambda_\mathrm{x}[\rho, \Pi, |\nabla\rho|, |\nabla\Pi|] = (1 - \lambda)E_\mathrm{x}[\rho, \Pi, |\nabla\rho|, |\nabla\Pi|] \tag{17}$$

The correlation contribution to the complement OTPD functional can be obtained through uniform coordinate scaling of the density as[29,30,52]

$$\begin{aligned}&\bar{E}^\lambda_\mathrm{c}[\rho, \Pi, |\nabla\rho|, |\nabla\Pi|] \\ &\quad= E_\mathrm{c}[\rho, \Pi, |\nabla\rho|, |\nabla\Pi|] - E^\lambda_\mathrm{c}[\rho, \Pi, |\nabla\rho|, |\nabla\Pi|] \\ &\quad= E_\mathrm{c}[\rho, \Pi, |\nabla\rho|, |\nabla\Pi|] \\ &\qquad - \lambda^2 E_\mathrm{c}[\rho^{1/\lambda}, \Pi^{1/\lambda}, |\nabla\rho^{1/\lambda}|, |\nabla\Pi^{1/\lambda}|]\end{aligned} \tag{18}$$

in which the scaled density and OTPD functions are defined as[63]

$$\rho^{1/\lambda}(\mathbf{r}) = (1/\lambda^3)\rho(\mathbf{r}/\lambda) \tag{19}$$

$$\Pi^{1/\lambda}(\mathbf{r}) = (1/\lambda^6)\Pi(\mathbf{r}/\lambda) \tag{20}$$

Sharkas, Toulouse, and Savin demonstrated numerically[29] that single-parameter multiconfigurational hybrid density functionals yield results of similar quality when ignoring such density scaling relations. Following ref 30, we neglect these relations for the total density and OTPD in the correlation complement functional and define

$$\bar{E}^\lambda_\mathrm{c}[\rho, \Pi, |\nabla\rho|, |\nabla\Pi|] = (1 - \lambda^2)E_\mathrm{c}[\rho, \Pi, |\nabla\rho|, |\nabla\Pi|] \tag{21}$$

Using eqs 17 and 21, the $\lambda$-MC-PDFT energy expression takes its final form

$$\begin{aligned}E_{\lambda\text{-MC-PDFT}} = {}& 2h^i_i + h^t_u\,{}^1D^t_u + E_\mathrm{H} \\ &+ \lambda\left(\frac{1}{2}\nu^{tv}_{uw}[{}^2\Delta^{tv}_{uw} - {}^1D^t_w\,{}^1D^v_u] - \nu^{tu}_{ii}\,{}^1D^t_u - \nu^{ii}_{jj}\right) \\ &+ (1 - \lambda)E_\mathrm{x}[\rho, \Pi, |\nabla\rho|, |\nabla\Pi|] \\ &+ (1 - \lambda^2)E_\mathrm{c}[\rho, \Pi, |\nabla\rho|, |\nabla\Pi|]\end{aligned} \tag{22}$$

where, for $\lambda = 0$ or $\lambda = 1$, the $\lambda$-MC-PDFT energy expression reduces to that corresponding to MC-PDFT or the underlying multiconfiguration reference method, respectively.

We note that the presence of the two-cumulant in eqs 14 and 22 opens the possibility of double counting of electron correlation, as some of the correlation effects captured by this quantity may also be described by the correlation complement functional. In eq 22, the two-cumulant and correlation functional appear with factors of $\lambda$ and $(1 - \lambda^2)$, respectively. As such, with an appropriately chosen correlation functional and mixing parameter, this issue of double counting can, in principle, be mitigated. However, we have no formal guarantee that double counting is completely absent in the formalism. We also note that, because the kinetic energy contribution is evaluated using a correlated 1-RDM, both $\lambda$-MC-PDFT and its parent MC-PDFT formalism have the potential to double count some kinetic correlation effects. The good numerical performance of MC-PDFT demonstrated in prior studies, however, suggests that this issue may not cause significant difficulties.

## 3. RESULTS AND DISCUSSION

The RDMs that enter the MC-PDFT and $\lambda$-MC-PDFT equations were obtained from v2RDM-driven CASSCF calculations performed using a plugin[64] to the Psi4 electronic structure package;[65] the active space RDMs, which satisfy either the PQG or PQG+T2 N-representability conditions, were optimized according to a boundary-point semidefinite programming (SDP) algorithm[66,67] similar to those described in refs 43 and 68. Both the MC-PDFT and $\lambda$-MC-PDFT procedures, along with the translated and fully translated versions of the SVWN3,[69−71] PBE,[72] and BLYP[73,74] XC functionals, have also been implemented in a plugin to Psi4.[75,76]

**3.1. $N_2$ and $H_2O$ Bond Dissociations.** In this section, we consider the accuracy of MC-PDFT and $\lambda$-MC-PDFT for describing the dissociation of $N_2$ and the double dissociation of $H_2O$; the nonparallelity errors (NPEs) in the respective potential energy curves (PECs), which are obtained by comparing the MC-PDFT and $\lambda$-MC-PDFT results with those from complete active-space second-order perturbation theory (CASPT2), serve as a useful metric in this context. The

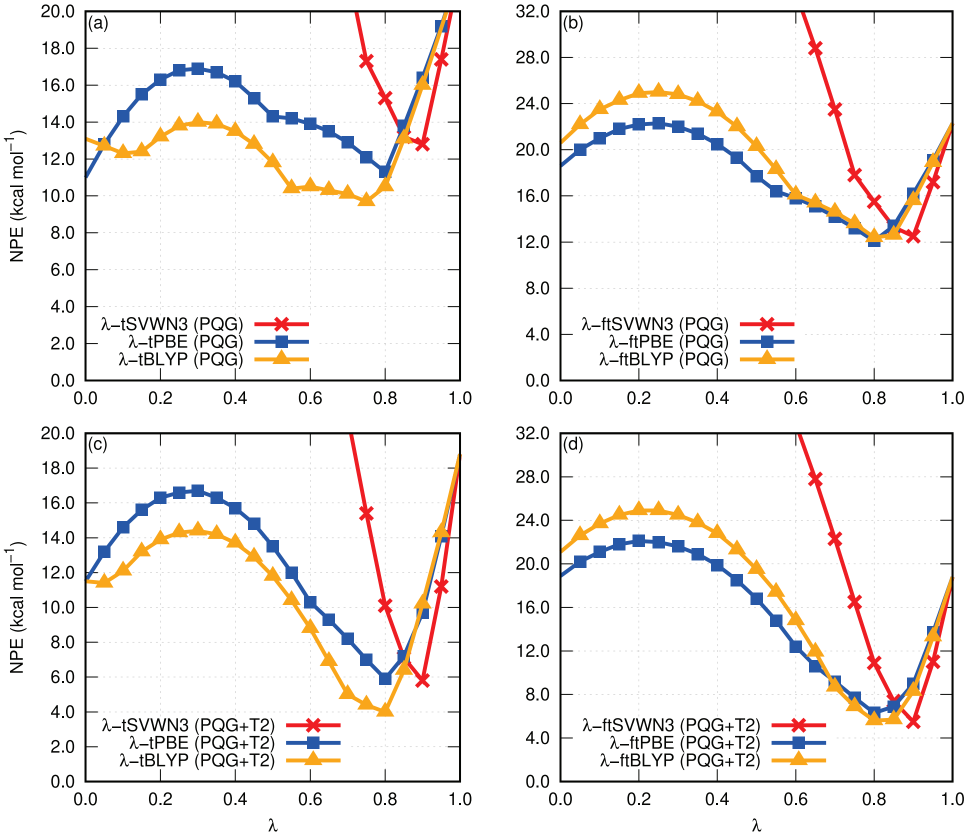

**Figure 1.** NPE in the dissociation curves for the $N_2$ molecule as a function of the mixing parameter, $\lambda$, when using PQG (a, b) or PQG+T2 (c, d) N-representability conditions and translated (a, c) or fully translated (b, d) $\lambda$-MC-PDFT functionals.

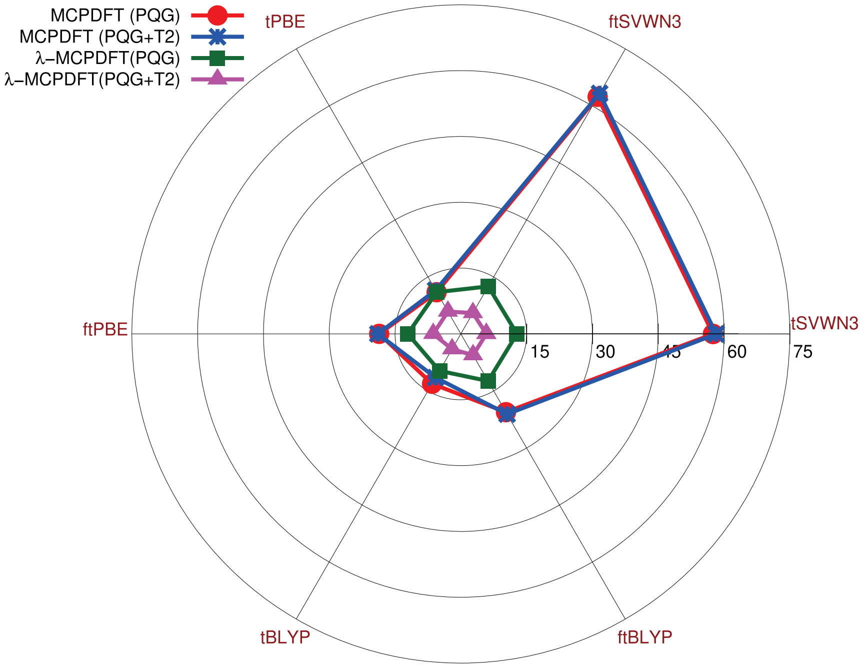

**Figure 2.** MC-PDFT and $\lambda$-MC-PDFT NPEs (kcal mol$^{-1}$) associated with the dissociation of $N_2$. The mixing parameter for $\lambda$-MC-PDFT is chosen to be that which gives the lowest NPE for each functional considered in Figure 1. Each concentric ring denotes an additional 15 kcal mol$^{-1}$ error.

CASSCF calculations underlying CASPT2, MC-PDFT, and $\lambda$-MC-PDFT employed full-valence active spaces and the cc-pVTZ basis set,[77] and, in the case of v2RDM-driven CASSCF, the ERI tensor was represented within the density-fitting (DF) approximation,[78,79] using the cc-pVTZ-JK auxiliary basis set.[80] All MC-PDFT and $\lambda$-MC-PDFT computations also employed the DF approximation. The CASPT2 computations were performed using the OPEN-MOLCAS electronic structure package,[81] and the standard imaginary shift[82] of 0.20 $E_h$ and

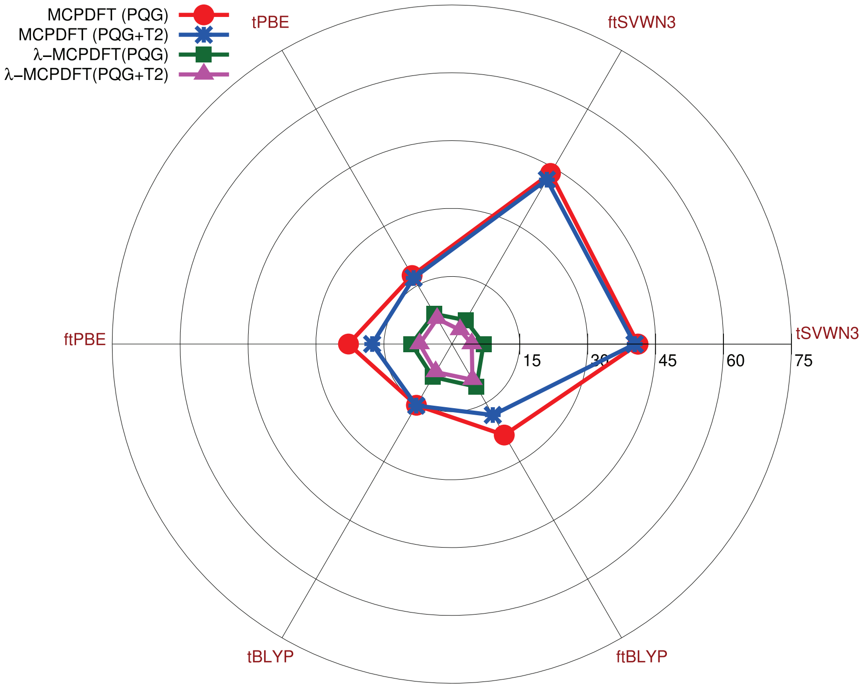

**Figure 3.** MC-PDFT and $\lambda$-MC-PDFT NPEs (kcal mol$^{-1}$) associated with the double dissociation of $H_2O$. The mixing parameter for $\lambda$-MC-PDFT is chosen to be that which gives the lowest NPE for each functional. Each concentric ring denotes an additional 15 kcal mol$^{-1}$ error.

Open-MOLCAS's default value of 0.25 $E_h$ for the IPEA shift[83] were applied throughout.

Figure 1 illustrates the effect of the mixing parameter, $\lambda$, on the NPE for $N_2$ when enforcing the PQG or PQG+T2 N-representability conditions and adopting either translated or fully translated $\lambda$-MC-PDFT functionals. The NPE is defined as the difference in the maximum and the minimum deviations between the $\lambda$-MC-PDFT and CASPT2 PECs from an N−N distance of 0.7 Å to an N−N distance of 5.0 Å. With the exception of that for tPBE combined with the PQG N-representability conditions, all NPE curves presented in Figure 1 exhibit their minimal value between $\lambda$ = 0.70 and 0.90. Specifically, when enforcing the PQG (PQG+T2) N-representability conditions and adopting tSVWN3, tPBE, tBLYP, ftSVWN3, ftPBE, and ftBLYP functionals, the optimal $\lambda$ values are 0.90 (0.90), 0.00 (0.80), 0.75 (0.80), 0.90 (0.90), 0.80 (0.80), and 0.80 (0.80), respectively. For tPBE/PQG, it appears that the optimal $\lambda$ value is 0.00 in this case, although the NPE at $\lambda$ = 0.80 is only 0.3 kcal mol$^{-1}$ larger. Note that the optimal values of the mixing parameters in all other cases lie between $\lambda$ = 0.70 and 0.90, which are close to the value of $\lambda$ = 0.75 used within the pCCD-$\lambda$DFT-based study of $N_2$ dissociation presented in ref 32.

Figure 2 presents the NPEs associated with the MC-PDFT and hybrid $\lambda$-MC-PDFT PECs, using the optimal $\lambda$ values identified for each functional/N-representability combination considered in Figure 1, and the data reveal several interesting features. First, as noted in ref 40, for both translated and fully translated MC-PDFT functionals, the NPE is somewhat insensitive to the N-representability of the RDMs. On the other hand, $\lambda$-MC-PDFT clearly yields lower NPE values when the underlying RDMs satisfy both the PQG and T2 conditions; it appears that the consideration of nonlocal exchange effects alleviates enough of the functional error to allow us to discern the error associated with approximate N-representability of the reference RDMs. Second, while the NPEs vary significantly with the choice of MC-PDFT functional, nonlocal exchange effects serve as a great equalizer; the NPE are quite similar for all $\lambda$-MC-PDFT methods, when enforcing a given set of N-representability conditions. Unsurprisingly, the improvement in the NPEs is largest for the $\lambda$-tSVWN3 and $\lambda$-ftSVWN3 functionals. Third, as observed in ref 40, the choice of translated or fully translated functionals does not significantly affect the NPE associated with functionals within either the MC-PDFT or $\lambda$-MC-PDFT formalisms. Fully translated functionals yield slightly lower NPE values than translated functionals, but this difference is far less significant than the improvements afforded by the admixture of nonlocal exchange effects.

Similar trends are observed for the NPEs associated with the $H_2O$ double-dissociation PEC. Figure 3 depicts the NPE for each functional, where the mixing parameter is chosen to minimize the $\lambda$-MC-PDFT NPE between O−H bond distances of 0.6 and 5.0 Å. In this case, when enforcing the PQG (PQG+T2) N-representability conditions and adopting tSVWN3, tPBE, tBLYP, ftSVWN3, ftPBE, and ftBLYP functionals, the optimal $\lambda$ values are 0.70 (0.70), 0.45 (0.50), 0.45 (0.50), 0.70 (0.70), 0.50 (0.50), and 0.50 (0.50), respectively. Relative to the case of $N_2$, the optimal mixing parameters, in general, are smaller for this problem. The only exception is tPBE, where the optimal value of $\lambda$ = 0.45 is clearly larger than the optimal value for $N_2$ dissociation (0.0). We again note that the inclusion of nonlocal exchange effects significantly reduces the NPEs, in general, and the variation in the performance of $\lambda$-MC-PDFT functionals is much less than that of the MC-PDFT functionals. In contrast to the case of $N_2$, the quality of the NPEs associated with $\lambda$-MC-PDFT functionals is less dependent upon the N-representability of the underlying RDMs. The NPEs for each $\lambda$-MC-PDFT functional, as a function of the mixing parameter, and PECs generated using the optimal values for the mixing parameter are illustrated in the Supporting Information.

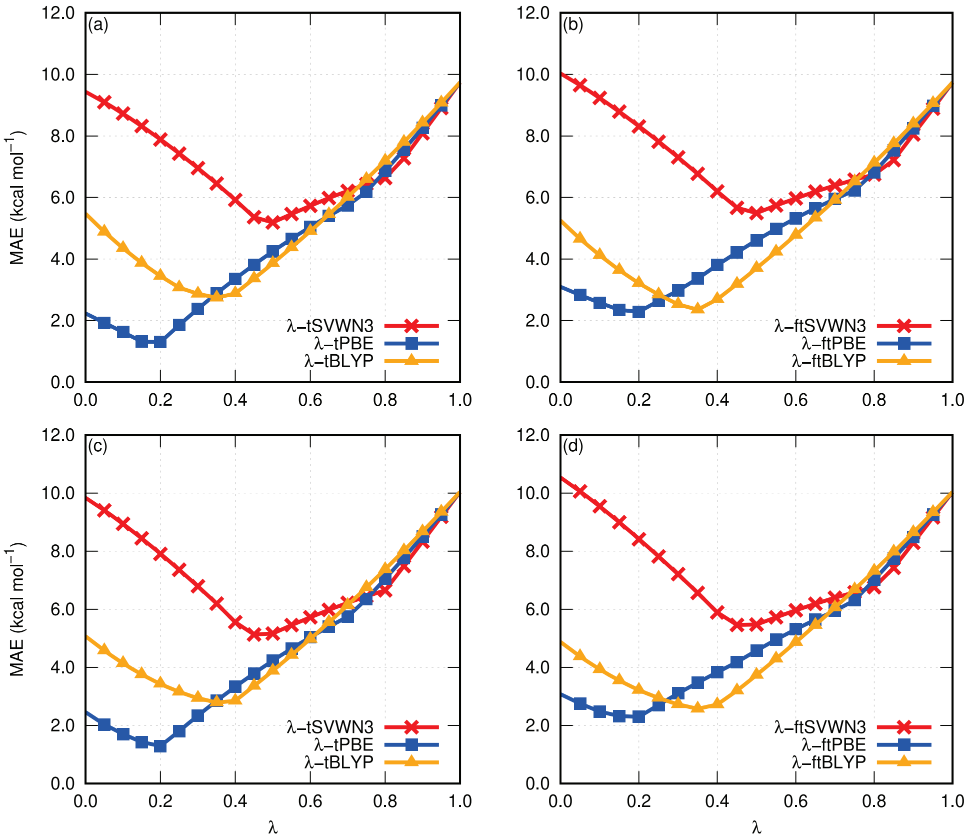

**Figure 4.** MAE (kcal mol$^{-1}$) in calculated O3ADD6 energies as a function of the mixing parameter, $\lambda$, when RDMs satisfy PQG (a, b) and PQG +T2 (c, d) N-representability conditions and when adopting translated (a, c) and fully translated (b, d) $\lambda$-MC-PDFT functionals.

**Table 1. Calculated Relative Energies (kcal mol$^{-1}$) of the Stationary Points and Separated Reactant Molecules That Comprise the O3ADD6 Dataset**

| | | | $O_3 + C_2H_2 \rightarrow$ | | | $O_3 + C_2H_4 \rightarrow$ | | | |
|---|---|---|---|---|---|---|---|---|---|
| method | N-representability | $\lambda$[a] | vdW | TS | cycloadd. | vdW | TS | cycloadd. | MAE |
| $\lambda$-tPBE | PQG | 0.20 | −0.42 | 7.84 | −67.75 | −2.19 | 4.91 | −57.66 | 1.30 |
| $\lambda$-tBLYP | | 0.35 | 0.24 | 12.51 | −61.41 | −2.70 | 8.82 | −56.18 | 2.75 |
| $\lambda$-tSVWN3 | | 0.50 | −1.15 | 7.72 | −73.88 | −5.72 | 4.69 | −72.34 | 5.19 |
| v2RDM-CASSCF | | 1.00 | 0.55 | 23.33 | −56.41 | −6.93 | 18.97 | −69.54 | 9.73 |
| $\lambda$-tPBE | PQG + T2 | 0.20 | −0.40 | 7.69 | −68.00 | −1.86 | 4.87 | −57.57 | 1.29 |
| $\lambda$-tBLYP | | 0.35 | 0.27 | 12.82 | −61.51 | −1.97 | 9.23 | −55.88 | 2.78 |
| $\lambda$-tSVWN3 | | 0.45 | −1.26 | 6.92 | −75.19 | −4.51 | 4.10 | −71.78 | 5.13 |
| v2RDM-CASSCF | | 1.00 | 0.63 | 25.86 | −55.60 | −4.19 | 21.55 | −68.13 | 10.04 |
| MC1H-PBE[b] | | 0.25 | −1.08 | 3.66 | −70.97 | −1.25 | 0.13 | −61.26 | 3.35 |
| MC1H-BLYP[b] | | 0.25 | −0.36 | 6.74 | −63.76 | −0.47 | 2.57 | −54.21 | 1.30 |
| reference values[c] | | | −1.90 | 7.74 | −63.80 | −1.94 | 3.37 | −57.15 | |

[a] The optimal mixing parameter. [b] From ref 30. [c] Best estimates from ref 85.

### 3.2. O3ADD6 Benchmark Set.

The O3ADD6 benchmark set is composed of the energies of several stationary points associated with the 1,3-dipolar cycloadditions of ozone ($O_3$) to ethylene ($C_2$H4) and $O_3$ to acetylene ($C_2$H2), relative to the energies of the isolated reactants. The stationary points [the van der Waals complex (vdW), the transition state (TS), and the cycloadduct (cycloadd.)] and the separated reactants are all assumed to be in singlet spin states. These systems present a challenge to quantum chemical methods, as the highest-occupied molecular orbital (HOMO) → lowest-unoccupied molecular orbital (LUMO) double excitation character in $O_3$ and the near-degeneracy of the $\pi$ and $\pi^*$ orbitals corresponding to the reactive $\pi$ bonds in the olefins result in strong MR character in several of the species along the reaction coordinate.[30,84] Here, we apply the MC-PDFT and $\lambda$-MC-PDFT methods to this data set, using the aug-cc-pVTZ basis set[77] and geometries for the stationary points given in ref 85. All v2RDM-driven CASSCF and $\lambda$-MC-PDFT calculations employed the DF approximation to the ERI tensor and the aug-cc-pVTZ-JK auxiliary basis set. To compare our results with those from refs 30 and 85, we consider active spaces composed of 2 electrons in 2 orbitals [denoted as (2e,2o)] for the reactants and (4e,4o) active spaces for the vdW, TS, and cycloadd. species; the orbitals comprising each active space are defined in ref 30. Following refs 85 and 30, we neglect vibrational zero-point energy contributions to the energies of the stationary points and separated reactants.

We identify the optimal nonlocal exchange mixing parameter, specific to the O3ADD6 benchmark set, for several $\lambda$-MC-PDFT functionals by minimizing the mean absolute error (MAE) in the relative energies of the stationary points and the isolated reactant molecules. The reference values to which the calculated relative energies are compared are taken from ref 85. Figure 4 depicts the MAEs in the calculated relative energies as a function of $\lambda$, and the data clearly convey the importance of nonlocal exchange effects for this problem, particularly in the case of $\lambda$-tSVWN3 and $\lambda$-ftSVWN3. For all functionals considered, the inclusion of some fraction of nonlocal exchange is beneficial, although this fraction is, in general, smaller than the optimal fraction for minimizing the NPE in the $N_2$ and $H_2O$ dissociation curves considered above. The optimal $\lambda$ values, which are tabulated in Table 1 and in the Supporting Information, are insensitive to the choice of N-representability conditions. The only functional that requires a different mixing parameter under different N-representability conditions is tSVWN3, and this value only changes by 0.05 in this case. One possible reason for this insensitivity is the small size of the active spaces considered. For example, for the (2e,2o) active space, the two-particle conditions alone are sufficient to yield ensemble-state N-representable RDMs.

While the v2RDM-driven CASSCF method can capture nondynamical correlation effects that are important in the systems comprising the O3ADD6 set, the large average errors associated with the approach (9.73 and 10.04 kcal mol$^{-1}$ when the calculations are performed under the PQG and PQG+T2 N-representability conditions, respectively) reflect its inability to describe dynamical electron correlation. These effects are well described by MC-PDFT and $\lambda$-MC-PDFT; each hybrid functional considered here, as well as the base MC-PDFT functionals (aside from tSVWN3 and ftSVWN3, see Supporting Information), substantially reduce the error associated with CASSCF. In particular, the admixture of 20% nonlocal exchange into the translated PBE OTPD functional reduces the MAE to only 1.30 kcal mol$^{-1}$ (PQG) or 1.29 kcal mol$^{-1}$ (PQG+T2), which is close to the 1.0 kcal mol$^{-1}$ threshold for "chemical accuracy." The description of the O3ADD6 afforded by $\lambda$-MC-PDFT with this functional is similar in quality to that exhibited by the MC1H-BLYP approach of ref 30 and superior to that displayed by the MC1H-PBE approach of that same work.

We note that the quality of the $\lambda$-MC-PDFT results, like that of the v2RDM-driven CASSCF, is independent of the N-representability of the underlying RDMs, in this case. As mentioned above, the likely reason for this behavior is the small size of the active spaces employed. Both sets of conditions we consider yield exact CASSCF RDMs for systems with (2e,2o) active spaces, and the (4e,4o) active spaces are not so large that we would expect significant differences to arise between RDMs satisfying the PQG and PQG+T2 conditions. We also note that full translation of the OTPD functionals does not necessarily lead to a reduction in the MAEs associated with MC-PDFT or $\lambda$-MC-PDFT. For example, a fully translated PBE functional with a 20% admixture of nonlocal exchange (the optimal value for this fully translated functional) performs slightly worse than the corresponding translated functional; the MAE in this case is 2.28 kcal mol$^{-1}$. A complete set of O3ADD6 relative energies and MAEs for translated and fully translated MC-PDFT and $\lambda$-MC-PDFT can be found in the Supporting Information.

## 4. CONCLUSIONS

We have presented a one-parameter global hybrid extension of the multiconfiguration pair density functional theory approach, inspired by the multiconfigurational one-parameter hybrid DFT developed in ref 30. Like MC1H, $\lambda$-MC-PDFT relies upon a linear decomposition of the electron−electron interaction operator to incorporate a fraction of nonlocal exchange into the MC-PDFT formalism. Unlike MC1H, $\lambda$-MC-PDFT is not a self-consistent theory, and the functionals we employ are functionals of the total density and on-top pair density, whereas the those employed in ref 30 are standard functionals of the total density and spin density. In both of these respects, the present approach is similar to the pCCD-$\lambda$DFT of ref 31, with the principal distinctions unique to this work being the source of the reference on-top pair densities and the fact that $\lambda$-MC-PDFT can, in principle, be applied to arbitrary total spin states, while pCCD-$\lambda$DFT is a closed-shell theory.

Not surprisingly, the admixture of nonlocal exchange improves the quality of the MC-PDFT energy, as measured by NPEs in molecular dissociation curves and the performance of the approach when applied to the O3ADD6 benchmark data set. It should be emphasized, however, that the results presented herein represent a best-possible scenario for the accuracy of $\lambda$-MC-PDFT, in that the mixing parameter is system-dependent and chosen specifically to minimize the error for the case in question. A universally useful $\lambda$-MC-PDFT formalism would require a single mixing parameter optimized over a large data set, as is done in Kohn−Sham DFT-based global hybrid schemes. Alternatively, the accuracy of the approach could be improved, in principle, by choosing a local mixing function,[15−17,24,25] $f(\mathbf{r})$, as opposed to a constant value $\lambda$, which could be defined in terms of the total density and the OTPD; we believe that this strategy may be the most promising path toward a general MC-PDFT-based formalism that incorporates nonlocal exchange effects. In addition, the MC-PDFT formalism could be further improved by generalizing the OTPD functionals to consider range separation of the coulomb interaction (see ref 32, for example) or double hybridization.

As mentioned above, $\lambda$-MC-PDFT is not a self-consistent method. This choice was motivated, in part, by technical considerations. The SDP algorithm we employ in the v2RDM-driven CASSCF that underlies $\lambda$-MC-PDFT assumes a linear objective function; complete self-consistency in v2RDM-based $\lambda$-MC-PDFT would require an SDP algorithm suitable for nonlinear objective functions,[86,87] which would be orders of magnitude less computationally efficient than the linear solver we currently employ.[68] Regardless, as long as the total density and OTPD derived from CASSCF are qualitatively correct, the lack of self-consistency should not be problematic,[32] as the associated errors have been shown to be smaller than those associated with the use of approximate functionals in MR+DFT methods.[88] Notable exceptions would be cases for which an approximate (i.e., v2RDM-driven) CASSCF yields qualitatively incorrect densities. In ref 40, we demonstrated that v2RDM-driven CASSCF calculations yield an incorrect dissociation limit for $CN^-$; challenges associated with heteronuclear dissociations are well-known in the context of v2RDM-based methods.[89] MC-PDFT built upon incorrect v2RDM-CASSCF densities, not surprisingly, also fails in this case. The admixture of nonlocal exchange does not improve this situation, as $\lambda$-MC-PDFT simply interpolates between two incorrect limits (see Supporting Information). This case should serve as a reminder that both MC-PDFT and $\lambda$-MC-PDFT are only as reliable as the densities obtained from the underlying MR approach.

Lastly, we highlight one unfortunate formal aspect of $\lambda$-MC-PDFT. One of the nice properties of MC-PDFT is that, unlike some other MR+DFT methods, it avoids double counting of electron correlation within the active space. This is achieved by retaining the classical Coulomb energy from CASSCF and relying on OTPD functionals for nonclassical contributions to the electron−electron interaction energy. However, upon introducing a nonzero exchange mixing parameter, $\lambda$, this property is formally lost in $\lambda$-MC-PDFT. The two-cumulant in eq 14 introduces some correlation effects within the active space that may also be described by the OTPD functional. Because both correlation contributions appear with $\lambda$-dependent scaling factors, an appropriately chosen value for the mixing parameter may partially address this issue. Presumably, double counting is minimized along with the total error in any fitting procedure used to determine $\lambda$, but we cannot formally guarantee that this is the case.

## ■ ASSOCIATED CONTENT

### Supporting Information

The Supporting Information is available free of charge at https://pubs.acs.org/doi/10.1021/acs.jctc.9b01178.

> Potential energy curves for the dissociation of molecular nitrogen and the symmetric double dissociation of water, nonparallelity errors for the double dissociation of water at several levels of theory, relative energies of the stationary points and separated reactant molecules that comprise the O3ADD6 data set, and potential energy curves for the dissociation of $CN^-$ (PDF)

## ■ AUTHOR INFORMATION

### Corresponding Author

**A. Eugene DePrince III** − *Department of Chemistry and Biochemistry, Florida State University, Tallahassee, Florida 32306-4390, United States;* orcid.org/0000-0003-1061-2521; Email: deprince@chem.fsu.edu

### Authors

**Mohammad Mostafanejad** − *Department of Chemistry and Biochemistry, Florida State University, Tallahassee, Florida 32306-4390, United States*

**Marcus Dante Liebenthal** − *Department of Chemistry and Biochemistry, Ithaca College, Ithaca, New York 14850, United States*

Complete contact information is available at: https://pubs.acs.org/10.1021/acs.jctc.9b01178

### Notes

The authors declare no competing financial interest.

## ■ ACKNOWLEDGMENTS

This material is based upon work supported by the Army Research Office Small Business Technology Transfer (STTR) program under Grants W911NF-16-C-0124 and W911NF-19-C0048. Mohammad Mostafanejad was supported by a fellowship from The Molecular Sciences Software Institute under NSF Grant ACI-1547580. We also thank the National Science Foundation Research Experiences for Undergraduates (NSF REU) Sites program, which supported this work under National Science Foundation Grant No. CHE-1659661

## ■ REFERENCES

(1) Helgaker, T.; Jørgensen, P.; Olsen, J. *Molecular Electronic−Structure Theory*; Wiley, 2000.

(2) Szabo, A.; Ostlund, N. S. *Modern Quantum Chemistry: Introduction to Advanced Electronic Structure Theory*; Dover Publications, 1996.

(3) Hohenberg, P.; Kohn, W. Inhomogeneous Electron Gas. *Phys. Rev.* **1964**, *136*, B864−B871.

(4) Kohn, W.; Sham, L. J. Self-consistent equations including exchange and correlation effects. *Phys. Rev.* **1965**, *140*, A1133−A1138.

(5) Lie, G. C.; Clementi, E. Study of the electronic structure of molecules. XXI. Correlation energy corrections as a functional of the HartreeFock density and its application to the hydrides of the second row atoms. *J. Chem. Phys.* **1974**, *60*, 1275−1287.

(6) Lie, G. C.; Clementi, E. Study of the electronic structure of molecules. XXII. Correlation energy corrections as a functional of the Hartree Fock type density and its application to the homonuclear diatomic molecules of the second row atoms. *J. Chem. Phys.* **1974**, *60*, 1288−1296.

(7) Pérez-Jiménez, A. J.; Pérez-Jordá, J. M. Combining multiconfigurational wave functions with correlation density functionals: A size-consistent method based on natural orbitals and occupation numbers. *Phys. Rev. A: At., Mol., Opt. Phys.* **2007**, *75*, 012503.

(8) Colle, R.; Salvetti, O. Approximate calculation of the correlation energy for the closed and open shells. *Theor. Chim. Acta* **1979**, *53*, 55−63.

(9) Moscardó, F.; San-Fabián, E. Density-functional formalism and the two-body problem. *Phys. Rev. A: At., Mol., Opt. Phys.* **1991**, *44*, 1549−1553.

(10) Paziani, S.; Moroni, S.; Gori-Giorgi, P.; Bachelet, G. B. Local-spin-density functional for multideterminant density functional theory. *Phys. Rev. B: Condens. Matter Mater. Phys.* **2006**, *73*, 155111.

(11) Gusarov, S.; Malmqvist, P.; Lindh, R.; Roos, B. O. Correlation potentials for a multiconfigurational-based density functional theory with exact exchange. *Theor. Chem. Acc.* **2004**, *112*, 84−94.

(12) Gusarov, S.; Malmqvist, P.-Å.; Lindh, R. Using on-top pair density for construction of correlation functionals for multideterminant wave functions. *Mol. Phys.* **2004**, *102*, 2207−2216.

(13) Takeda, R.; Yamanaka, S.; Yamaguchi, K. CAS-DFT based on odd-electron density and radical density. *Chem. Phys. Lett.* **2002**, *366*, 321−328.

(14) Stoll, H. On the coupling of multi-configuration self-consistent-field and density-functional information. *Chem. Phys. Lett.* **2003**, *376*, 141−147.

(15) Gräfenstein, J.; Cremer, D. The combination of density functional theory with multi-configuration methods CAS-DFT. *Chem. Phys. Lett.* **2000**, *316*, 569−577.

(16) Gräfenstein, J.; Cremer, D. Development of a CAS-DFT method covering non-dynamical and dynamical electron correlation in a balanced way. *Mol. Phys.* **2005**, *103*, 279−308.

(17) Miehlich, B.; Stoll, H.; Savin, A. A correlation-energy density functional for multideterminantal wavefunctions. *Mol. Phys.* **1997**, *91*, 527−536.

(18) Grimme, S.; Waletzke, M. A combination of Kohn−Sham density functional theory and multi-reference configuration interaction methods. *J. Chem. Phys.* **1999**, *111*, 5645.

(19) Wu, W.; Shaik, S. VB-DFT: a nonempirical hybrid method combining valence bond theory and density functional energies. *Chem. Phys. Lett.* **1999**, *301*, 37−42.

(20) Pollet, R.; Savin, A.; Leininger, T.; Stoll, H. Combining multideterminantal wave functions with density functionals to handle

near-degeneracy in atoms and molecules. *J. Chem. Phys.* **2002**, *116*, 1250−1258.

(21) Leininger, T.; Stoll, H.; Werner, H.-J.; Savin, A. Combining long-range configuration interaction with short-range density functionals. *Chem. Phys. Lett.* **1997**, *275*, 151−160.

(22) Malcolm, N. O.; McDouall, J. J. Combining multiconfigurational wave functions with density functional estimates of dynamic electron correlation. *J. Phys. Chem.* **1996**, *100*, 10131−10134.

(23) Kraka, E. Homolytic dissociation energies from GVB-LSDC calculations. *Chem. Phys.* **1992**, *161*, 149−153.

(24) Gritsenko, O. V.; van Meer, R.; Pernal, K. Efficient evaluation of electron correlation along the bond-dissociation coordinate in the ground and excited ionic states with dynamic correlation suppression and enhancement functions of the on-top pair density. *Phys. Rev. A: At., Mol., Opt. Phys.* **2018**, *98*, 062510.

(25) Gritsenko, O. V.; Pernal, K. Complete active space and corrected density functional theories helping each other to describe vertical electronic $\pi \rightarrow \pi^*$ excitations in prototype multiple-bonded molecules. *J. Chem. Phys.* **2019**, *151*, 024111.

(26) Gagliardi, L.; Truhlar, D. G.; Li Manni, G.; Carlson, R. K.; Hoyer, C. E.; Bao, J. L. Multiconfiguration Pair-Density Functional Theory: A New Way To Treat Strongly Correlated Systems. *Acc. Chem. Res.* **2017**, *50*, 66−73.

(27) Li Manni, G.; Carlson, R. K.; Luo, S.; Ma, D.; Olsen, J.; Truhlar, D. G.; Gagliardi, L. Multiconfiguration pair-density functional theory. *J. Chem. Theory Comput.* **2014**, *10*, 3669−3680.

(28) Ghosh, S.; Verma, P.; Cramer, C. J.; Gagliardi, L.; Truhlar, D. G. Combining Wave Function Methods with Density Functional Theory for Excited States. *Chem. Rev.* **2018**, *118*, 7249−7292.

(29) Sharkas, K.; Toulouse, J.; Savin, A. Double-hybrid density-functional theory made rigorous. *J. Chem. Phys.* **2011**, *134*, 064113.

(30) Sharkas, K.; Savin, A.; Jensen, H. J. A.; Toulouse, J. A multiconfigurational hybrid density-functional theory. *J. Chem. Phys.* **2012**, *137*, 044104.

(31) Garza, A. J.; Bulik, I. W.; Henderson, T. M.; Scuseria, G. E. Synergy between pair coupled cluster doubles and pair density functional theory. *J. Chem. Phys.* **2015**, *142*, 044109.

(32) Garza, A. J.; Bulik, I. W.; Henderson, T. M.; Scuseria, G. E. Range separated hybrids of pair coupled cluster doubles and density functionals. *Phys. Chem. Chem. Phys.* **2015**, *17*, 22412−22422.

(33) Ying, F.; Zhou, C.; Zheng, P.; Luan, J.; Su, P.; Wu, W. $\lambda$-Density Functional Valence Bond: A Valence Bond-Based Multiconfigurational Density Functional Theory With a Single Variable Hybrid Parameter. *Front. Chem.* **2019**, *7*, 225.

(34) Toulouse, J.; Sharkas, K.; Brémond, E.; Adamo, C. Communication: Rationale for a new class of double-hybrid approximations in density-functional theory. *J. Chem. Phys.* **2011**, *135*, 101102.

(35) Roos, B. O.; Taylor, P. R.; Sigbahn, P. E.M. A complete active space SCF method (CASSCF) using a density matrix formulated super-CI approach. *Chem. Phys.* **1980**, *48*, 157−173.

(36) Roos, B. O. *Advances in Chemical Physics*; John Wiley & Sons, Inc., 1987; Vol. *68*; pp 399−445.

(37) Siegbahn, P.; Heiberg, A.; Roos, B.; Levy, B. A comparison of the super-CI and the Newton−Raphson scheme in the complete active space SCF method. *Phys. Scr.* **1980**, *21*, 323−327.

(38) Siegbahn, P. E. M.; Almlöf, J.; Heiberg, A.; Roos, B. O. The complete active space SCF (CASSCF) method in a Newton−Raphson formulation with application to the HNO molecule. *J. Chem. Phys.* **1981**, *74*, 2384−2396.

(39) Becke, A. D.; Savin, A.; Stoll, H. Extension of the local-spin-density exchange-correlation approximation to multiplet states. *Theor. Chem. Acc.* **1995**, *91*, 147−156.

(40) Mostafanejad, M.; DePrince, A. E. Combining Pair-Density Functional Theory and Variational Two-Electron Reduced-Density Matrix Methods. *J. Chem. Theory Comput.* **2019**, *15*, 290−302.

(41) Mazziotti, D. A. Variational minimization of atomic and molecular ground-state energies via the two-particle reduced density matrix. *Phys. Rev. A: At., Mol., Opt. Phys.* **2002**, *65*, 062511.

(42) Gidofalvi, G.; Mazziotti, D. A. Active-space two-electron reduced-density-matrix method: Complete active-space calculations without diagonalization of the N-electron Hamiltonian. *J. Chem. Phys.* **2008**, *129*, 134108.

(43) Fosso-Tande, J.; Nguyen, T.-S.; Gidofalvi, G.; DePrince, A. E., III Large-Scale Variational Two-Electron Reduced-Density-Matrix-Driven Complete Active Space Self-Consistent Field Methods. *J. Chem. Theory Comput.* **2016**, *12*, 2260−2271.

(44) Cohen, A. J.; Mori-Sánchez, P.; Yang, W. Insights into current limitations of density functional theory. *Science* **2008**, *321*, 792−794.

(45) Becke, A. D. Density-functional thermochemistry. I. The effect of the exchangeonly gradient correction. *J. Chem. Phys.* **1992**, *96*, 2155−2160.

(46) Becke, A. D. Density-functional thermochemistry. II. The effect of the Perdew-Wang generalizedgradient correlation correction. *J. Chem. Phys.* **1992**, *97*, 9173−9177.

(47) Becke, A. D. Densityfunctional thermochemistry.III. The role of exactexchange. *J. Chem. Phys.* **1993**, *98*, 5648.

(48) Becke, A. D. A new mixing of Hartree-Fock and local density-functional theories. *J. Chem. Phys.* **1993**, *98*, 1372−1377.

(49) Becke, A. D. Density-functional thermochemistry. IV. A new dynamical correlation functional and implications for exact-exchange mixing. *J. Chem. Phys.* **1996**, *104*, 1040−1046.

(50) Giuliani, G.; Vignale, G. *Quantum Theory of the Electron Liquid*; Cambridge University Press: Cambridge, 2005.

(51) Bao, J. L.; Wang, Y.; He, X.; Gagliardi, L.; Truhlar, D. G. Multiconfiguration Pair-Density Functional Theory Is Free from Delocalization Error. *J. Phys. Chem. Lett.* **2017**, *8*, 5616−5620.

(52) Kalai, C.; Toulouse, J. A general range-separated double-hybrid density-functional theory. *J. Chem. Phys.* **2018**, *148*, 164105.

(53) Coleman, A. J. Structure of Fermion Density Matrices. *Rev. Mod. Phys.* **1963**, *35*, 668−686.

(54) Husimi, K. Some Formal Properties of the Density Matrix. *Proceedings of the Physico-Mathematical Society of Japan. 3rd Series* **1940**, *22*, 264−314.

(55) Mayer, J. E. Electron Correlation. *Phys. Rev.* **1955**, *100*, 1579−1586.

(56) Löwdin, P.-O. Quantum Theory of Many-Particle Systems. I. Physical Interpretations by Means of Density Matrices, Natural Spin-Orbitals, and Convergence Problems in the Method of Configurational Interaction. *Phys. Rev.* **1955**, *97*, 1474−1489.

(57) Carlson, R. K.; Truhlar, D. G.; Gagliardi, L. Multiconfiguration Pair-Density Functional Theory: A Fully Translated Gradient Approximation and Its Performance for Transition Metal Dimers and the Spectroscopy of $Re_2Cl_8^{2-}$. *J. Chem. Theory Comput.* **2015**, *11*, 4077−4085.

(58) Garrod, C.; Percus, J. K. Reduction of the N-particle variational problem. *J. Math. Phys.* **1964**, *5*, 1756−1776.

(59) Zhao, Z.; Braams, B. J.; Fukuda, M.; Overton, M. L.; Percus, J. K. The reduced density matrix method for electronic structure calculations and the role of three-index representability conditions. *J. Chem. Phys.* **2004**, *120*, 2095−2104.

(60) Erdahl, R. M. Representability. *Int. J. Quantum Chem.* **1978**, *13*, 697−718.

(61) Mazziotti, D. A. Approximate solution for electron correlation through the use of Schwinger probes. *Chem. Phys. Lett.* **1998**, *289*, 419−427.

(62) DePrince, A. E.; Mazziotti, D. A. Cumulant reconstruction of the three-electron reduced density matrix in the anti-Hermitian contracted Schrödinger equation. *J. Chem. Phys.* **2007**, *127*, 104104.

(63) Higuchi, M.; Higuchi, K. Pair density functional theory. *Comput. Theor. Chem.* **2013**, *1003*, 91−96.

(64) For v2RDM-CASSCF, v0.8, a variational two-electron reduced-density-matrix-driven approach to complete active space self-consistent field theory, see https://github.com/edeprince3/v2rdm_casscf (accessed 2018).

(65) Turney, J. M.; Simmonett, A. C.; Parrish, R. M.; Hohenstein, E. G.; Evangelista, F. A.; Fermann, J. T.; Mintz, B. J.; Burns, L. A.; Wilke, J. J.; Abrams, M. L.; Russ, N. J.; Leininger, M. L.; Janssen, C. L.; Seidl,

E. T.; Allen, W. D.; Schaefer, H. F.; King, R. A.; Valeev, E. F.; Sherrill, C. D.; Crawford, T. D. Psi4: an Open-Source Ab Initio Electronic Structure Program. *WIRES Comput. Mol. Sci.* **2012**, *2*, 556−565.

(66) Povh, J.; Rendl, F.; Wiegele, A. A Boundary Point Method to Solve Semidefinite Programs. *Computing* **2006**, *78*, 277−286.

(67) Malick, J.; Povh, J.; Rendl, F.; Wiegele, A. Regularization Methods for Semidefinite Programming. *SIAM Journal on Optimization* **2009**, *20*, 336−356.

(68) Mazziotti, D. A. Large-Scale Semidefinite Programming for Many-Electron Quantum Mechanics. *Phys. Rev. Lett.* **2011**, *106*, 083001.

(69) Gáspár, R. Statistical exchange for electron in shell and the$X\alpha$ method. *Acta Phys. Acad. Sci. Hung.* **1974**, *35*, 213−218.

(70) Slater, J. C. A simplification of the Hartree-Fock method. *Phys. Rev.* **1951**, *81*, 385−390.

(71) Vosko, S. H.; Wilk, L.; Nusair, M. Accurate spin-dependent electron liquid correlation energies for local spin density calculations: a critical analysis. *Can. J. Phys.* **1980**, *58*, 1200−1211.

(72) Perdew, J. P.; Burke, K.; Ernzerhof, M. Generalized gradient approximation made simple. *Phys. Rev. Lett.* **1996**, *77*, 3865−3868.

(73) Becke, A. D. Density-functional exchange-energy approximation with correct asymptotic behavior. *Phys. Rev. A: At., Mol., Opt. Phys.* **1988**, *38*, 3098−3100.

(74) Lee, C.; Yang, W.; Parr, R. G. Development of the Colle-Salvetti correlation-energy formula into a functional of the electron density. *Phys. Rev. B: Condens. Matter Mater. Phys.* **1988**, *37*, 785−789.

(75) https://github.com/edeprince3/RDM-inoles.

(76) https://github.com/SinaMostafanejad/OpenRDM.

(77) Dunning, T. H. Gaussian basis sets for use in correlated molecular calculations. I. The atoms boron through neon and hydrogen. *J. Chem. Phys.* **1989**, *90*, 1007−1023.

(78) Whitten, J. L. Coulombic potential energy integrals and approximations. *J. Chem. Phys.* **1973**, *58*, 4496−4501.

(79) Dunlap, B. I.; Connolly, J. W. D.; Sabin, J. R. On some approximations in applications of $X\alpha$ theory. *J. Chem. Phys.* **1979**, *71*, 3396.

(80) Weigend, F. A fully direct RI-HF algorithm: Implementation, optimized auxiliary basis sets, demonstration of accuracy and efficiency. *Phys. Chem. Chem. Phys.* **2002**, *4*, 4285−4291.

(81) Aquilante, F.; Autschbach, J.; Carlson, R. K.; Chibotaru, L. F.; Delcey, M. G.; De Vico, L.; Fdez. Galván, I.; Ferré, N.; Frutos, L. M.; Gagliardi, L.; Garavelli, M.; Giussani, A.; Hoyer, C. E.; Li Manni, G.; Lischka, H.; Ma, D.; Malmqvist, P. Å.; Müller, T.; Nenov, A.; Olivucci, M.; Pedersen, T. B.; Peng, D.; Plasser, F.; Pritchard, B.; Reiher, M.; Rivalta, I.; Schapiro, I.; Segarra-Martí, J.; Stenrup, M.; Truhlar, D. G.; Ungur, L.; Valentini, A.; Vancoillie, S.; Veryazov, V.; Vysotskiy, V. P.; Weingart, O.; Zapata, F.; Lindh, R. Molcas 8: New capabilities for multiconfigurational quantum chemical calculations across the periodic table. *J. Comput. Chem.* **2016**, *37*, 506−541.

(82) Forsberg, N.; Malmqvist, P.-Å. Multiconfiguration perturbation theory with imaginary level shift. *Chem. Phys. Lett.* **1997**, *274*, 196−204.

(83) Ghigo, G.; Roos, B. O.; Malmqvist, P. Å. A modified definition of the zeroth-order Hamiltonian in multiconfigurational perturbation theory (CASPT2). *Chem. Phys. Lett.* **2004**, *396*, 142−149.

(84) Wheeler, S. E.; Ess, D. H.; Houk, K. N. Thinking out of the black box: Accurate barrier heights of 1,3-dipolar cycloadditions of ozone with acetylene and ethylene. *J. Phys. Chem. A* **2008**, *112*, 1798−1807.

(85) Zhao, Y.; Tishchenko, O.; Gour, J. R.; Li, W.; Lutz, J. J.; Piecuch, P.; Truhlar, D. G. Thermochemical Kinetics for Multireference Systems: Addition Reactions of Ozone. *J. Phys. Chem. A* **2009**, *113*, 5786−5799.

(86) Nascimento, D. R.; DePrince, A. E., III Spatial and Spin Symmetry Breaking in Semidefinite-Programming-Based Hartree-Fock Theory. *J. Chem. Theory Comput.* **2018**, *14*, 2418−2426.

(87) Mazziotti, D. A. Realization of Quantum Chemistry without Wave Functions through First-Order Semidefinite Programming. *Phys. Rev. Lett.* **2004**, *93*, 213001.

(88) Stoll, H.; Savin, A. *Density Functional Theory Methods in Physics*; Dreizler, R. M., da Providencia, J., Eds; Plenum: New York, 1985; p 177.

(89) Van Aggelen, H.; Bultinck, P.; Verstichel, B.; Van Neck, D.; Ayers, P. W. Incorrect diatomic dissociation in variational reduced density matrix theory arises from the flawed description of fractionally charged atoms. *Phys. Chem. Chem. Phys.* **2009**, *11*, 5558−5560.

## ■ NOTE ADDED AFTER ASAP PUBLICATION

This paper was published ASAP on March 9, 2020, with errors in the Table of Contents/Abstract graphic. The corrected version was reposted on March 11, 2020.